

This is the accepted manuscript made available via CHORUS, the article has been published as:

## Resonance decay contributions to higher-order anisotropic flow coefficients

Zhi Qiu, Chun Shen, and Ulrich Heinz

Phys. Rev. C **86**, 064906 — Published 19 December 2012

DOI: [10.1103/PhysRevC.86.064906](https://doi.org/10.1103/PhysRevC.86.064906)



ciency for the iterative determination of the QGP shear viscosity.

The analysis presented here uses final states generated with the (2+1)-dimensional boost-invariant viscous hydrodynamic code **VISH2+1** for 200 A GeV Au+Au collisions at the Relativistic Heavy-Ion Collider (RHIC) and for 2.76 A TeV Pb+Pb collisions at the Large Hadron Collider (LHC) at various collision centralities, with previously determined [11, 19, 34] hydrodynamic input parameters. We find very similar results at both collision energies and therefore show here only plots for LHC collisions. Since the decay contributions from different resonances to the mentioned observables depend only on their decay channels and transverse momentum distributions, we expect little sensitivity to the assumption of longitudinal boost-invariance implicit in our approach and expect our reordered resonance decay tables to perform equally well for both (2+1)-d and (3+1)-d hydrodynamic simulations, and for a wide range of input parameters (such as QGP viscosity, thermalization time, initial entropy and energy density, etc.).

## II. RESONANCE ORDERING

The momentum distributions of directly emitted (“thermal”) resonances of species  $i$  are computed from the Cooper-Frye formula [53]:

$$E \frac{dN_i}{d^3 p} = \frac{dN}{dy p_T dpt d\phi_p} = \frac{g_i}{(2\pi)^3} \int_{\Sigma} p^\mu d^3 \sigma_\mu (f_{i0} + \delta f_i). \quad (1)$$

Here  $\Sigma$  is the hydro-to-hadron conversion hypersurface,  $d^3 \sigma_\mu$  its surface normal vector,  $f_{i0} = 1/[e^{\beta(p-u-\mu_i)} \mp 1]$  is the Bose or Fermi thermal equilibrium distribution function, and  $\delta f_i$  accounts for viscous corrections (driven by the viscous pressure tensor  $\pi_{\mu\nu}(x)$  on the conversion surface) of the local phase-space distribution along  $\Sigma$ . We assume the quadratic form  $\delta f = \frac{1}{2} f_0 (1 \pm f_0) \frac{p^\mu p^\nu}{T^2} \frac{\pi_{\mu\nu}}{(e+p)}$ .

Resonance decays increase the total yields of the stable hadrons and change their momentum distributions. For kinematic reasons, most of the light decay daughters have low transverse momenta, thus modifying the shape of light stable hadrons (pions, kaons) particle spectra mostly in the region  $p_T < 1.5$  GeV [54]. We denote the total decay contribution to the momentum distribution of stable hadron species  $i$  by  $\delta(dN_i/(dyd^2p_T))$ , and the total spectrum (obtained by adding this to the thermally emitted spectrum  $dN_i^{\text{th}}/(dyd^2p_T)$ ) by  $dN_i^{\text{tot}}/(dyd^2p_T)$ . (We here include only strong and electromagnetic decays.) The  $p_T$ -integrated total yield  $\delta(dN_i/dy)$  of decay products of species  $i$  is denoted by  $\delta N_i$ , with  $N_i^{\text{tot}} = N_i^{\text{th}} + \delta N_i = N_i^{\text{th}} + \sum_j \tilde{b}_{j \rightarrow i} N_j^{\text{th}}$ , where the sum is over resonances  $j$  and  $\tilde{b}_{j \rightarrow i}$  is the effective branching ratio (see Eq. (4) below) for the decay  $j \rightarrow i$ .

The contribution to  $\delta N_i$  from a particular resonance  $j$  is not only influenced by its mass (through the Boltzmann suppression factor  $\sim e^{-E_j/T}$ ), but also by its spin

degeneracy factor  $g_j$  and its branching ratio  $\tilde{b}_{j \rightarrow i}$  into the decay channel that feeds stable particle species  $i$ . For each stable hadron species  $i$  it is therefore a different set of resonances that makes the most important contributions. Our goal is to order the resonances in decreasing order of importance, for each stable particle species  $i$ . We here assume that the conversion surface has constant temperature  $T_{\text{conv}}$ . The different hadron resonances have  $T_{\text{conv}}$ -dependent non-equilibrium fugacities  $\lambda_j$  that ensure constant stable particle ratios equal to their chemical equilibrium values at  $T_{\text{chem}}$  and  $\mu_B = 0$ , independent of the hydro-to-hadron conversion temperature  $T_{\text{conv}}$ . While the actual fractions contributed by each resonance to the stable particle yields depend on  $T_{\text{conv}}$ , the ordering of these fractions is largely  $T_{\text{conv}}$ -independent.

We start from the resonance table in the **AZHYDRO** package,<sup>1</sup> which includes 319 species of hadrons (counting different isospin states such as  $\pi^+$ ,  $\pi^0$ ,  $\pi^-$  as separate species) with rest masses up to 2.25 GeV. After fixing the value of  $T_{\text{conv}}$  we look up the non-equilibrium fugacity  $\lambda_j$  for each of these 319 species from the EOS s95p-PCE tables constructed in Ref. [56]. For each stable particle species  $i$  we then generate an ordered list of resonances  $j$  that can decay directly into  $i$ . Note that in this ordering we account not only for direct decay contribution but also for multi-step decay cascades, where  $j$  first decays into an unstable resonance  $k$  which further decays (directly or through more intermediate steps) into the stable species  $i$ .

Table I shows the beginning of this contribution table for positively charged pions, for a conversion temperature  $T_{\text{conv}} = 120$  MeV. The “total contribution” percentages  $c_{j \rightarrow i}$  in the third column are computed as

$$c_{j \rightarrow i} = \frac{N_i^{(j)}}{\sum_{j'} N_i^{(j')}} = \frac{\tilde{b}_{j \rightarrow i} N_j^{\text{th}}}{\sum_{j'} \tilde{b}_{j' \rightarrow i} N_{j'}^{\text{th}}}, \quad (2)$$

$$N_j^{\text{th}} = g_j m_j^2 \sum_{k=1}^{\infty} \frac{(\pm)^{k+1}}{k} \lambda_j^k K_2 \left( k \frac{m_j}{T} \right), \quad (3)$$

where the effective branching ratios  $\tilde{b}_{j \rightarrow i}$  in Eq. (2) account for multi-step decay cascades as follows:

$$\begin{aligned} \tilde{b}_{j \rightarrow i} &= b_{j \rightarrow i} + \sum_{k_1} b_{j \rightarrow k_1} b_{k_1 \rightarrow i} \\ &+ \sum_{k_1, k_2} b_{j \rightarrow k_1} b_{k_1 \rightarrow k_2} b_{k_2 \rightarrow i} + \dots \end{aligned} \quad (4)$$

The sum over  $k$  in (3) takes care of quantum statistical effects, with the upper (lower) sign for bosons (fermions). For all hadrons except pions accurate results can be obtained by keeping only the first term  $k=1$ , i.e. by ignoring quantum statistical effects. Even for pions, a few

<sup>1</sup> AZHYDRO is available at the URL <http://www.physics.ohio-state.edu/~froderma/>.

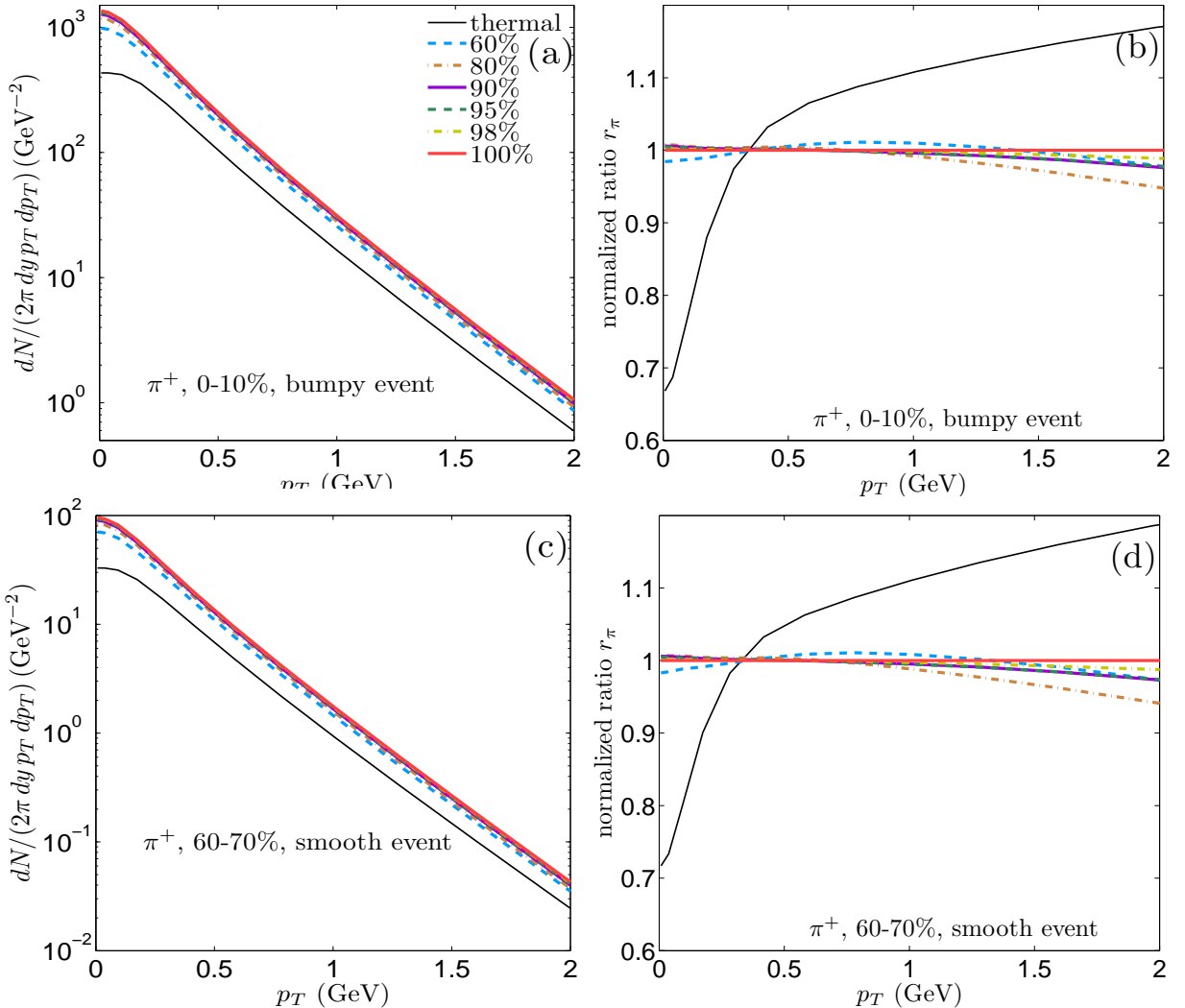


FIG. 1. (Color online) Transverse momentum spectra of  $\pi^+$ , for a bumpy central (0-10% centrality, top panels) and a smooth peripheral (60-70% centrality, bottom panels) Pb-Pb collision at LHC energies. Panels (a) and (c) present the absolutely normalized spectra, while panels (b) and (d) show the normalized ratio  $r_\pi(p_T)$  defined in Eq. (5). Different lines correspond to different cumulative resonance decay contributions between 0% (“thermal”) and 100%. See text for discussion.

name	mass (GeV)	total contribution (%)
$\omega$	0.78260	15.398
$\rho^0$	0.77580	11.179
$\rho^+$	0.77580	11.098
.....	.....	.....

TABLE I. Example of the  $\pi^+$  contribution table for  $T_{\text{conv}} = 120$  MeV.

$k$ -terms suffice for good precision (in our calculations we truncate the series in (3) at  $k=10$ ). The complete ordered resonance decay contribution tables for  $\pi^+$ ,  $K^+$ ,  $p$ ,  $\Lambda$ ,  $\Sigma^+$  and  $\Xi^-$  are given in the Appendix. Horizontal lines in the tables indicate where the cumulative resonance decay contributions  $c_i^{\text{cut}} = \sum_{j=1}^{j_{\text{cut}}} c_{j \rightarrow i}$  exceed cer-

tain threshold percentages (as indicated) of the total resonance decay contribution to species  $i$ .

In the following section we show the stable hadron  $p_T$ -spectra and their anisotropic flow coefficients as a function of these cumulative decay contribution percentages  $c_i^{\text{cut}}$ , in order to assess how many resonances from these ordered decay tables should be included for an accurate computation of these observables.

### III. RESULTS AND DISCUSSION

Using the ordered tables described in Sec. II and truncating the sum over resonance decay contributions at  $j_{\text{cut}}$  values corresponding to various different cumulative resonance decay contribution thresholds  $c_i^{\text{cut}}$ , we performed calculations for  $\pi^+$ ,  $K^+$ , and  $p$ . We tested individ-

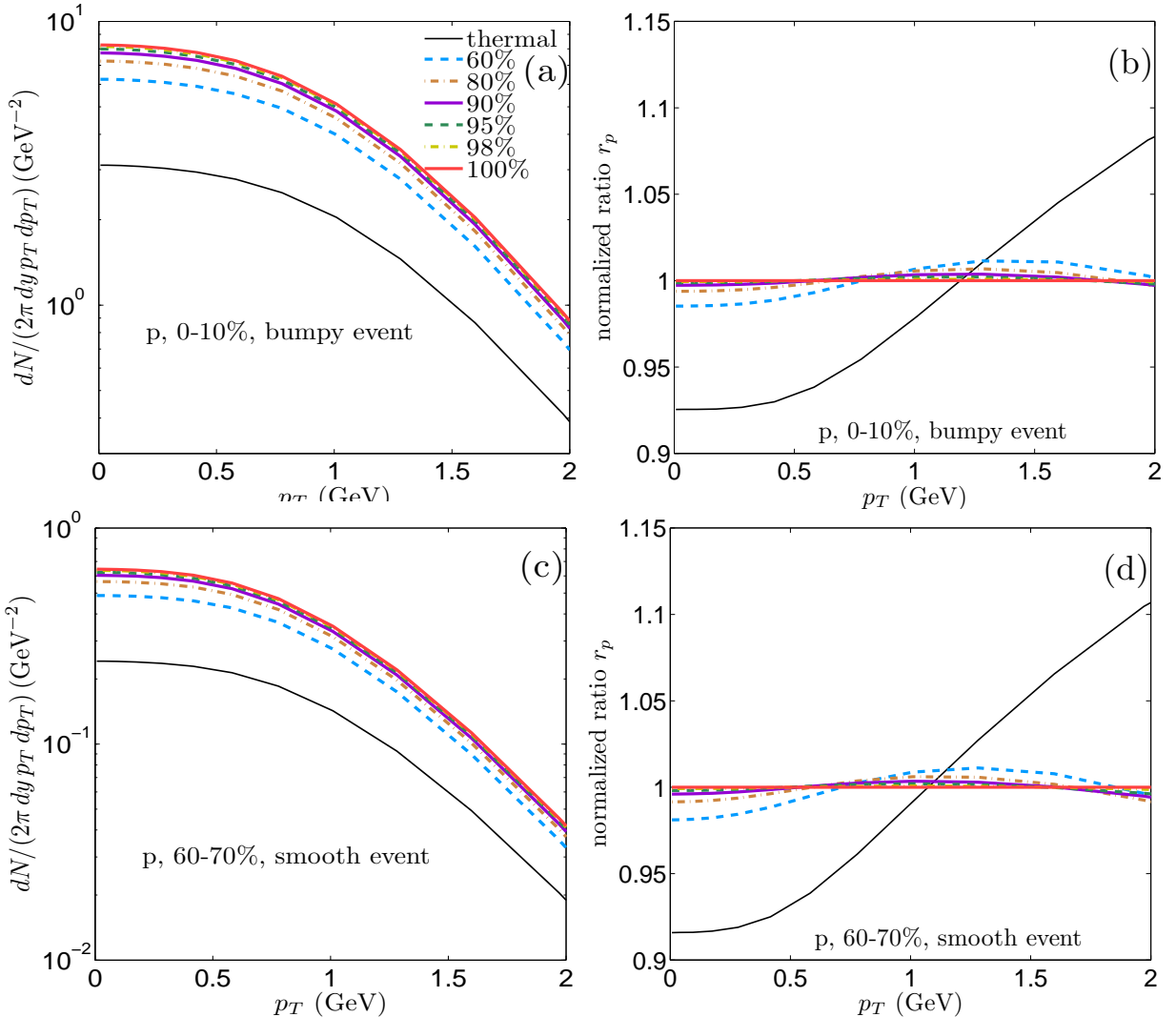


FIG. 2. (Color online) Same as Fig.1, but for protons.

ual bumpy as well as (ellipticity-aligned and ensemble-averaged) smooth initial conditions at both RHIC and LHC energies, for a variety of collision centralities. Since the results were found all to be qualitatively similar, we show only a small selection, focussing on pions and protons from one bumpy Pb-Pb event from the 0–10% centrality class and from the smooth averaged initial condition corresponding to the 60–70% centrality class, both at LHC energy ( $\sqrt{s}=2.76 \text{ A GeV}$ ).

Figure 1 shows the pion  $p_T$ -spectra, for the bumpy central collision in the upper panels and the smooth peripheral event in the lower panels. The left panels show the usual semilogarithmic plots of the absolutely normalized  $p_T$ -distribution. As is well-known, the directly emitted (“thermal”) pions constitute only about 50–60% of all observed pions, the rest coming from resonance decays. The “thermal” spectrum also has the wrong shape: resonance decay pions predominantly contribute to the low- $p_T$  part of the spectrum, making it steeper. However, this shape

difference between the truncated and full resonance decay spectrum disappears almost completely already when including only the 9 strongest decay channels, accounting for just 60% of the total pion yield from resonance decays. This is shown in the right panels of Fig. 1 where we plot the ratio

$$r_i(p_T) = \frac{\frac{dN_i^{\text{th}}}{dy dp_T} + \frac{1}{\sum_{j=1}^{j_{\text{cut}}} c_{j \rightarrow i}} \sum_{j=1}^{j_{\text{cut}}} \frac{dN_i^{(j)}}{dy dp_T}}{\frac{dN_i^{\text{th}}}{dy dp_T} + \sum_{j=1}^{j_{\text{max}}} \frac{dN_i^{(j)}}{dy dp_T}} \quad (5)$$

for  $i=\pi$  as a function of  $p_T$ . ( $N_i^{(j)}$  is the contribution to particle species  $i$  from decays of particle species  $j$  (see Eq. (2)), and  $j_{\text{max}}$  is the index of the last resonance in the ordered resonance decay table from Sec. II.) The numerator includes only resonance decays up to  $j_{\text{cut}}$ , but we renormalize those decay contributions by the cumulative decay contribution  $c_i^{\text{cut}}$  corresponding to the same  $j_{\text{cut}}$  value. ( $c_i^{\text{cut}}$  is easily calculated from Eqs. (2,3) and directly obtained by summing the entries in the third

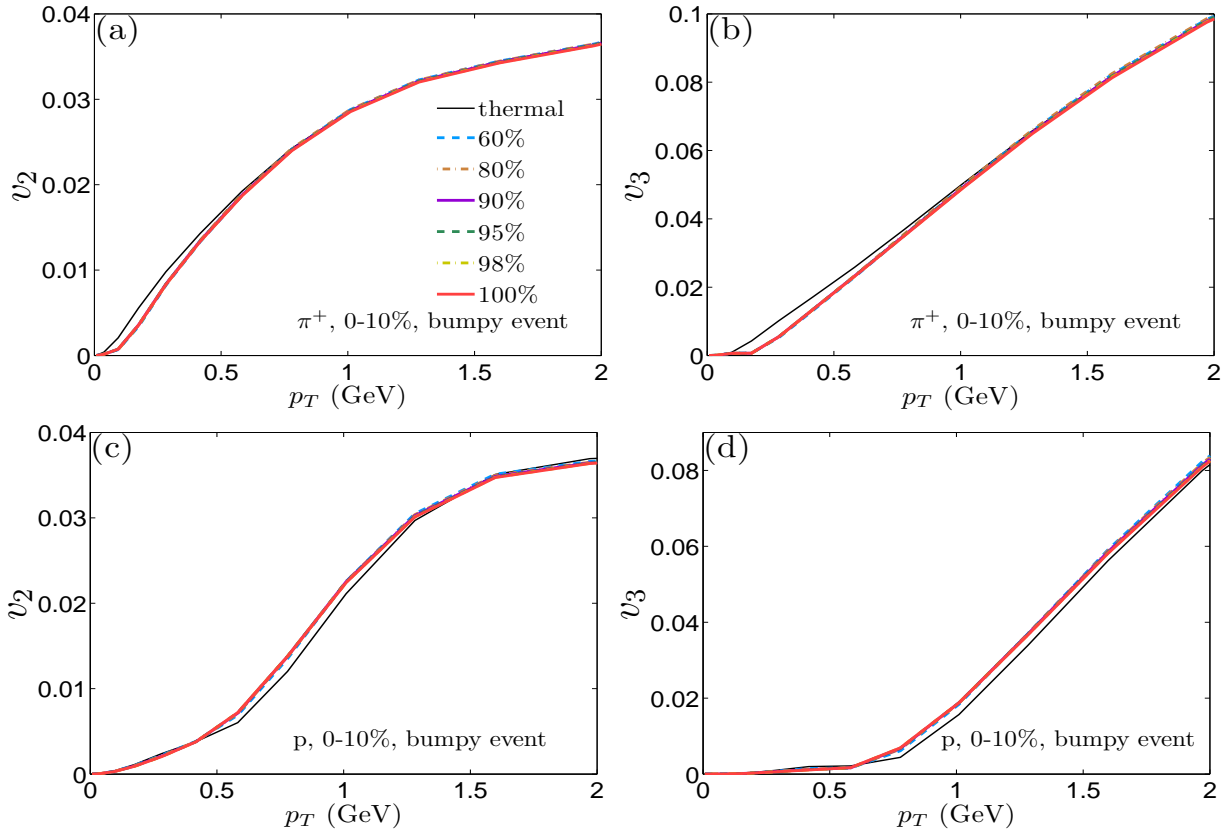


FIG. 3. (Color online) The differential elliptic ( $v_2$ , left panel) and triangular flow ( $v_3$ , right panel), for  $\pi^+$  (upper panels) and  $p$  (lower panels), for one bumpy Pb-Pb event from the 0–10% centrality class at LHC energy. As in Fig. 1, lines of different styles and colors correspond to different cumulative resonance decay fractions.

column of the resonance decay table.) This renormalization corrects for the missing yield from the truncation of the decay table. The remaining effect (after missing yield renormalization) of the truncation on the *shape* of the  $p_T$ -spectrum is seen in panels (b) and (d) of Fig. 1: Whereas without any resonance decays the ratio  $r_\pi(p_T)$  changes by almost a factor 2 between  $p_T = 0$  and 2 GeV, this variation is reduced to less than 5% already for  $c_\pi^{\text{cut}} = 60\%$ , for both bumpy and smooth initial conditions in both central and peripheral collisions.

In Fig. 2 we show in the same way the proton spectra. Again the shape of the spectra can be accurately reproduced by taking into account a small fraction of all decay contributions (note the expanded vertical scale in Figs. 2b,d): after renormalization to account for the missing yield, just the 4 strongest of 75 decay channels (three charge states of the  $\Delta(1232)$  resonance and one charge state of  $\Delta(1600)$ ), corresponding to 60% of the total resonance decay yield for protons, reproduce the full proton spectrum with < 5% error between  $p_T = 0$  and 2 GeV.

We conclude that, by accounting for the missing yield through appropriate renormalization, the correctly normalized total pion and proton spectra can be obtained, with shape errors < 5%, by including only the strongest decay channels accounting for the leading 60% of the to-

tal resonance decay yields. A quick look at the tables in the Appendix shows that this will reduce the number of resonance decays (and thus computer time) by at least a factor 10.

We now proceed to a discussion of the differential and  $p_T$ -integrated anisotropic flow coefficients  $v_n$ , defined by

$$v_n(p_T) e^{in\psi_n(p_T)} = \int d\phi_p e^{in\phi_p} \frac{dN}{dy p_T dp_T d\phi_p} / \frac{dN}{dy p_T dp_T},$$

$$v_n e^{in\psi_n} = \int p_T dp_T d\phi_p e^{in\phi_p} \frac{dN}{dy p_T dp_T d\phi_p} / \frac{dN}{dy}. \quad (6)$$

Here the spectrum  $dN/(dy p_T dp_T d\phi_p)$  includes all contributions from the ordered resonance decay table for the considered stable species up to a certain threshold  $j_{\text{cut}}$ , with the truncated resonance decay contribution renormalized for the missing yield by a factor  $1/c_i^{\text{cut}}$  as shown in the numerator of Eq. (5). In Figs. 3 and 4 below we specify the cumulative decay contribution percentage  $c_i^{\text{cut}}$  to indicate the truncation level corresponding to each curve.

Figure 3 shows the differential elliptic and triangular flows for pions and protons, for one single bumpy central (0–10% centrality) event. We see that once again excellent agreement with the full resonance decay calculation is already obtained when including only the small subset

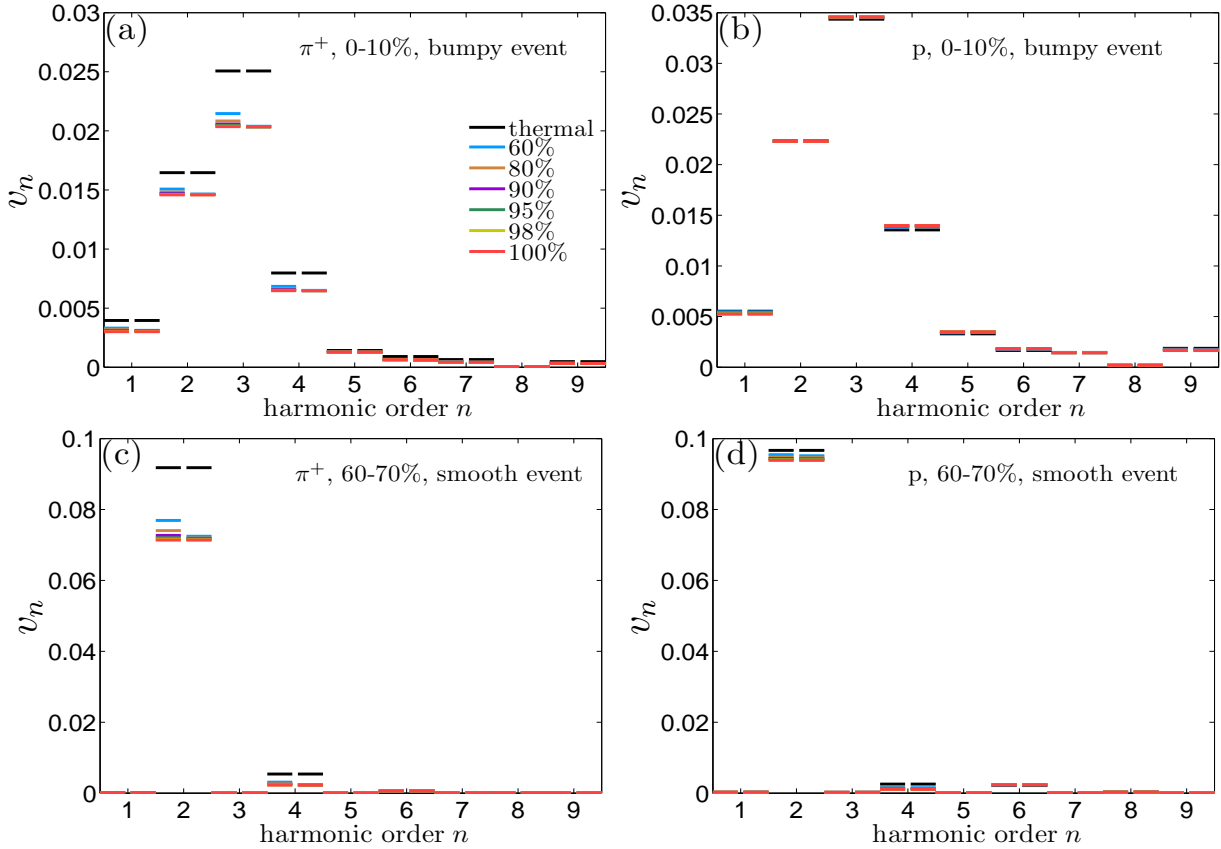


FIG. 4. (Color online) The  $p_T$ -integrated anisotropic flow coefficients  $v_n$ ,  $n=1,\dots,9$ , for  $\pi^+$  (a,c) and  $p$  (b,d), for a bumpy central (0-10%) collision event (a,b) and a smooth averaged peripheral (60-70%) collision event (c,d). Line colors and styles as in Figs. 1-3. For a discussion of the two sets of lines for each harmonic order  $n$  see text.

of resonances that account for the top 60% of the resonance decay yields. We checked that this result is generic, i.e. it does not depend on the selected event (although the elliptic and triangular flows do).

For the  $p_T$ -integrated harmonic flow coefficients  $v_n$  we show in Fig. 4 results for all harmonic orders from  $n=1$  to 9, again for pions and protons and for a bumpy central as well as a smooth peripheral event. For the smooth averaged initial condition, the odd harmonics vanish by symmetry. For fluctuating initial conditions, the  $v_n$  values shown here and their relative size depend on the randomly selected event. All plots shown in this paper are based on one and the same bumpy central collision event.

For each harmonic order  $n$ , Fig. 4 shows two sets of results. The left set corresponds to results obtained by using the truncated resonance decay spectra shown in Figs. 1a,c and 2a,c, without missing yield renormalization. The right set uses the renormalized truncated decay spectra as defined in the numerator of Eq. (5). One observes a much faster convergence towards the full result in the right sets than in the left sets. The reason is that, by renormalizing the truncated resonance decay contributions for the missing yield, the correct mixing ratio between direct thermal and indirect decay contributions is ensured and the shape of the total  $p_T$ -spectrum is approx-

imated much more accurately than without renormalization (see Figs. 1b,d and 2b,d). Figure 4 demonstrates that, when using the renormalized truncated decay spectra, accounting for just the top 60% decay contributions (i.e. including only the 9 strongest decay channels contributing to pions and the 4 strongest decay channels contributing to the proton spectra) reproduces the full results for the harmonic flow coefficients  $v_n$  with excellent precision: The lines corresponding to different  $c_i^{\text{cut}}$  values  $\geq 60\%$  are almost indistinguishable.

Future precision extractions of the QGP viscosity may require highly precise  $v_n$  values. For such a purpose one can adjust  $j_{\text{cut}}$  to include a larger fraction of all resonance decays if needed.

For a given precision, the required minimal  $j_{\text{cut}}$  truncation indices and cumulative resonance decay fractions  $c_K^{\text{cut}}$  for kaons lie between those for pions and protons. The  $c_i^{\text{cut}}$  for  $i=\pi, K, p$  are almost identical at RHIC and LHC energies, i.e. only weakly sensitive to radial flow.

#### IV. CONCLUSIONS

We have shown that for a sufficiently accurate determination of the differential anisotropic flow coefficients

$v_n(p_T)$  only those resonances need to be included that generate the top 60% of the largest decay contributions to the stable particle yields. For the single particle spectra, correct normalization of the total yield requires a renormalization of the truncated resonance decay yield as given in the numerator of Eq. (5). With this renormalization, good convergence of the slope of the pion spectra and of the  $p_T$ -integrated anisotropic flow coefficients  $v_n$  requires inclusion of only the 9 strongest contributing channels for pions and only the 4 strongest channels for protons, accounting in both cases for just 60% of the total decay yield. This reduces the number of resonance decay channels to be evaluated by a factor >10, without loss of precision, leading to a similar reduction of the total computing time for the final stable hadron distributions.

In hybrid model calculations [50] the late hadronic stage is described microscopically by a Boltzmann cascade that propagates a reduced set of resonances until final kinetic decoupling. In this case the spectra of all unstable resonances that are explicitly included in the Boltzmann cascade must be generated on the conversion surface. This is still only a small subset of all resonances included in the resonance decay tables. The optimal ordering of the resonance decay tables for the purpose of generating input for the late-stage Boltzmann cascade and the corresponding optimized truncation fractions  $c_i^{\text{cut}}$  will be studied in a follow-up report.

**Acknowledgments:** This work was supported by the U.S. Department of Energy under Grants No. DE-SC0004286 and (within the framework of the JET Collaboration) DE-SC0004104.

- 
- [1] P. F. Kolb, J. Sollfrank and U. Heinz, Phys. Rev. C **62**, 054909 (2000).
  - [2] D. Teaney, J. Lauret and E. V. Shuryak, Phys. Rev. Lett. **86**, 4783 (2001); and nucl-th/0110037.
  - [3] P. Huovinen, P. F. Kolb, U. Heinz, P. V. Ruuskanen and S. A. Voloshin, Phys. Lett. B **503**, 58 (2001).
  - [4] R. A. Lacey and A. Taranenko, PoS **CFRNC2006**, 021 (2006); R. A. Lacey *et al.*, Phys. Rev. Lett. **98**, 092301 (2007); A. Adare *et al.*, Phys. Rev. Lett. **98**, 172301 (2007); H.-J. Drescher, A. Dumitru, C. Gombeaud, and J.-Y. Ollitrault, Phys. Rev. C **76**, 024905 (2007). K. Dusling and D. Teaney, Phys. Rev. C **77**, 034905 (2008); Z. Xu, C. Greiner, and H. Stöcker, Phys. Rev. Lett. **101**, 082302 (2008); D. Molnar and P. Huovinen, J. Phys. G **35**, 104125 (2008); R. A. Lacey, A. Taranenko and R. Wei, in *Proc. 25th Winter Workshop on Nuclear Dynamics*, W. Bauer, R. Bellwied, and J.W. Harris (eds.), (EP Systema, Budapest, 2009) p. 73 [arXiv:0905.4368 [nucl-ex]]; K. Dusling, G. D. Moore, and D. Teaney, Phys. Rev. C **81**, 034907 (2010); A. K. Chaudhuri, J. Phys. G **37**, 075011 (2010); R. A. Lacey *et al.*, Phys. Rev. C **82**, 034910 (2010).
  - [5] T. Hirano, U. Heinz, D. Kharzeev, R. Lacey and Y. Nara, Phys. Lett. B **636**, 299 (2006).
  - [6] P. Romatschke and U. Romatschke, Phys. Rev. Lett. **99**, 172301 (2007).
  - [7] M. Luzum and P. Romatschke, Phys. Rev. C **78**, 034915 (2008).
  - [8] M. Luzum and P. Romatschke, Phys. Rev. Lett. **103**, 262302 (2009).
  - [9] H. Song and U. Heinz, Phys. Lett. B **658**, 279 (2008).
  - [10] H. Song and U. Heinz, Phys. Rev. C **77**, 064901 (2008). H. Song, PhD thesis, Ohio State University (2009) [arXiv:0908.3656 [nucl-th]].
  - [11] H. Song, S. A. Bass, U. Heinz, T. Hirano and C. Shen, Phys. Rev. Lett. **106**, 192301 (2011); and Phys. Rev. C **83**, 054910 (2011).
  - [12] M. Luzum, Phys. Rev. C **83**, 044911 (2011).
  - [13] R. A. Lacey, A. Taranenko, N. N. Ajitanand and J. M. Alexander, Phys. Rev. C **83**, 031901 (2011).
  - [14] P. Bozek, M. Chojnacki, W. Florkowski and B. Tomasik, Phys. Lett. **B694**, 238 (2010); P. Bozek, *ibid.* **B699**, 283 (2011).
  - [15] T. Hirano, P. Huovinen and Y. Nara, Phys. Rev. C **83**, 021902 (2011).
  - [16] B. Schenke, S. Jeon and C. Gale, Phys. Rev. Lett. **106**, 042301 (2011).
  - [17] B. Schenke, S. Jeon and C. Gale, Phys. Lett. **B702**, 59 (2011).
  - [18] H. Song, S. A. Bass and U. Heinz, Phys. Rev. C **83**, 054912 (2011).
  - [19] C. Shen, U. Heinz, P. Huovinen and H. Song, Phys. Rev. C **84**, 044903 (2011).
  - [20] U. Heinz, C. Shen, and H. Song, in *PANIC11*, AIP Conf. Proc., in press [arXiv:1108.5323 [nucl-th]].
  - [21] C. Shen and U. Heinz, Phys. Rev. C **85**, 054902 (2012) [arXiv:1202.6620 [nucl-th]].
  - [22] B. Alver and G. Roland, Phys. Rev. C **81**, 054905 (2010).
  - [23] A. Adare *et al.* (PHENIX Collaboration), arXiv:1105.3928 [nucl-ex]; R. Lacey *et al.* (PHENIX Collaboration), J. Phys. G **38**, 124048 (2011)
  - [24] P. Sorensen *et al.* (STAR Collaboration), J. Phys. G **38**, 124029 (2011)
  - [25] K. Aamodt *et al.* (ALICE Collaboration), Phys. Rev. Lett. **107**, 032301 (2011); R. Snellings *et al.* (ALICE Collaboration), J. Phys. G **38**, 124013 (2011); M. Krzewicki *et al.* (ALICE Collaboration), *ibid.* J. Phys. G **38**, 124047 (2011); K. Aamodt *et al.* (ALICE Collaboration), Phys. Lett. B **708**, 249 (2012).
  - [26] S. Chatrchyan *et al.* (CMS Collaboration), CERN preprint CMS-PAS-HIN-11-005; J. Velkovska *et al.* (CMS Collaboration), J. Phys. G **38**, 124011 (2011).
  - [27] P. Steinberg *et al.* (ATLAS Collaboration), J. Phys. G **38**, 124004 (2011) J. Jia *et al.* (ATLAS Collaboration), J. Phys. G **38**, 124012 (2011); G. Aad *et al.* (ATLAS Collaboration), Phys. Rev. C **86**, 014907 (2012).
  - [28] H. Holopainen, H. Niemi and K. J. Eskola, Phys. Rev. C **83**, 034901 (2011).
  - [29] G.-Y. Qin, H. Petersen, S. A. Bass and B. Müller, Phys. Rev. C **82**, 064903 (2010).
  - [30] Z. Qiu and U. Heinz, Phys. Rev. C **84**, 024911 (2011).
  - [31] K. Dusling, F. Gelis and R. Venugopalan, Nucl. Phys. **A872**, 161 (2011).
  - [32] C. Flensburg, arXiv:1108.4862 [nucl-th].

- [33] B. Schenke, S. Jeon and C. Gale, Phys. Rev. C **85**, 024901 (2012).
- [34] Z. Qiu, C. Shen and U. Heinz, Phys. Lett. B **707**, 151 (2012)
- [35] H. Petersen, R. La Placa and S. A. Bass, J. Phys. G **39**, 055102 (2012).
- [36] B. Schenke, P. Tribedy and R. Venugopalan, Phys. Rev. Lett. **108**, 252301 (2012).
- [37] P. Bozek and W. Broniowski, Phys. Rev. C **85**, 044910 (2012).
- [38] P. Mota and T. Kodama, Prog. Theor. Phys. Suppl. **193**, 315 (2012).
- [39] R. Chatterjee, H. Holopainen, T. Renk and K. J. Eskola, Phys. Rev. C **85**, 064910 (2012).
- [40] J. Jia and S. Mohapatra, arXiv:1203.5095 [nucl-th]; J. Jia and D. Teaney, arXiv:1205.3585 [nucl-ex].
- [41] L. Pang, Q. Wang and X. -N. Wang, Phys. Rev. C **86**, 024911 (2012).
- [42] P. Bozek, arXiv:1208.1887 [nucl-th].
- [43] H. Petersen, G.-Y. Qin, S. A. Bass and B. Müller, Phys. Rev. C **82**, 041901 (2010).
- [44] M. Luzum, Phys. Lett. **B696**, 499 (2011).
- [45] J. Xu and C. M. Ko, Phys. Rev. **C84**, 014903 (2011).
- [46] M. Luzum, J. Phys. G **38**, 124026 (2011)
- [47] C. Shen *et al.*, J. Phys. G **38**, 124045 (2011)
- [48] Z. Qiu and U. Heinz, AIP Conf. Proc. **1441**, 774 (2012).
- [49] Z. Qiu and U. W. Heinz, Phys. Lett. B **717**, 261 (2012) [arXiv:1208.1200 [nucl-th]].
- [50] H. Song, S. A. Bass and U. Heinz, Phys. Rev. C **83**, 024912 (2011).
- [51] J. Adams *et al.* [STAR Collaboration], Phys. Rev. Lett. **92**, 112301 (2004).
- [52] S. S. Adler *et al.* [PHENIX Collaboration], Phys. Rev. C **69**, 034909 (2004).
- [53] F. Cooper and G. Frye, Phys. Rev. D **10**, 186 (1974).
- [54] J. Sollfrank, P. Koch and U. Heinz, Phys. Lett. B **252**, 256 (1990); and Z. Phys. C **52**, 593 (1991).
- [55] P. Braun-Munzinger, K. Redlich and J. Stachel, in *Quark-Gluon Plasma 3*, R. C. Hwa and X.-N. Wang, eds. (World Scientific, Singapore, 2004), pp. 491-599 [nucl-th/0304013].
- [56] P. Huovinen and P. Petreczky, Nucl. Phys. **A837**, 26 (2010).
- [57] C. Shen, U. Heinz, P. Huovinen and H. Song, Phys. Rev. C **82**, 054904 (2010)
- [58] Y. -L. Yan, Y. Cheng, D. -M. Zhou, B. -G. Dong, X. Cai, B. -H. Sa and L. P. Csernai, arXiv:1110.6704 [nucl-th].
- [59] B. Schenke, S. Jeon and C. Gale, Phys. Rev. C **82**, 014903 (2010) [arXiv:1004.1408 [hep-ph]].
- [60] P. Bozek, arXiv:1110.6742 [nucl-th].

## V. APPENDIX: FEED DOWN CONTRIBUTION TABLES FOR $\pi$ , $K$ , $p$ , $\Lambda$ , $\Sigma^+$ , AND $\Xi^-$

name	mass (GeV)	total contribution (%)	
$\omega$	0.78259	15.398	
$\rho^0$	0.7758	11.179	
$\rho^+$	0.7758	11.098	
$K^{*+}(892)$	0.89166	5.54	
$\bar{K}^{*0}(892)$	0.8961	5.355	
$\eta$	0.54775	4.682	
$\bar{\Delta}^-(1232)$	1.232	2.613	
$\Delta^{++}(1232)$	1.232	2.606	
$b_1^+(1235)$	1.2295	2.498	60%
$\eta'(958)$	0.95778	2.069	
$a_0^+(980)$	0.9847	1.862	
$h_1(1170)$	1.17	1.26	
$a_1^+(1260)$	1.23	1.226	
$b_1^-(1235)$	1.2295	1.19	
$b_1^0(1235)$	1.2295	1.181	
$a_2^+(1320)$	1.3183	1.177	
$\Sigma^+(1385)$	1.3828	1.09	
$\bar{\Sigma}^-(1385)$	1.3872	1.057	
$f_1(1285)$	1.2818	0.994	
$\bar{K}_1^0(1270)$	1.273	0.963	
$K_1^+(1270)$	1.273	0.962	
$\bar{\Delta}^0(1232)$	1.232	0.857	
$\Delta^+(1232)$	1.232	0.856	
$a_1^0(1260)$	1.23	0.817	
$a_2^0(1320)$	1.3183	0.771	
$\phi(1020)$	1.0195	0.762	80%
$f_0(980)$	0.9741	0.613	
$K_1^0(1270)$	1.273	0.472	
$K_1^-(1270)$	1.273	0.472	
$f_2(1270)$	1.2754	0.45	
$a_1^-(1260)$	1.23	0.409	
$a_0^-(980)$	0.9847	0.402	
$a_0^0(980)$	0.9847	0.399	
$a_2^-(1320)$	1.3183	0.398	
$\pi_1^+(1400)$	1.376	0.373	
$K_2^{*+}(1430)$	1.4256	0.368	
$\Xi^0(1530)$	1.5318	0.357	
$\bar{\Delta}^-(1600)$	1.6	0.356	
$\Delta^{++}(1600)$	1.6	0.356	
$\bar{K}_2^{*0}(1430)$	1.4324	0.35	
$\bar{\Xi}^-(1530)$	1.535	0.347	
$\bar{K}_1^0(1400)$	1.402	0.341	
$K_1^+(1400)$	1.402	0.34	
$p(1520)$	1.52	0.305	
$\bar{n}(1520)$	1.52	0.305	
$\eta(1295)$	1.294	0.297	
$\bar{K}^{*-}(1410)$	1.414	0.294	
$K^{*+}(1410)$	1.414	0.294	

TABLE II. Resonance contribution list for  $\pi^+$ , for  $T_{\text{conv}} = 120 \text{ MeV}$ .

name	mass (GeV)	total contribution (%)
$\pi^+(1300)$	1.3	0.257
$\bar{\Delta}^0(1600)$	1.6	0.249
$\Delta^+(1600)$	1.6	0.249
$\bar{n}(1440)$	1.44	0.241
$p(1440)$	1.44	0.241
$\omega(1420)$	1.419	0.205
$a_0^+(1450)$	1.474	0.196
$\Lambda(1405)$	1.4065	0.188
		90%
$\bar{\Lambda}(1405)$	1.4065	0.188
$\eta_2(1645)$	1.617	0.185
$f_1(1420)$	1.4263	0.174
$K_1^0(1400)$	1.402	0.173
$K_1^-(1400)$	1.402	0.173
$a_0^0(1450)$	1.474	0.153
$\bar{n}(1675)$	1.675	0.147
$p(1675)$	1.675	0.147
$\bar{\Delta}^-(1700)$	1.7	0.145
$\Delta^{++}(1700)$	1.7	0.145
$\omega_3(1670)$	1.667	0.144
$\pi^0(1300)$	1.3	0.142
$K^{*0}(1410)$	1.414	0.14
$K^{*-}(1410)$	1.414	0.14
$\Delta^0(1600)$	1.6	0.135
$\bar{\Delta}^+(1600)$	1.6	0.134
$\rho_3^+(1690)$	1.6888	0.123
$p(1680)$	1.685	0.119
$\bar{n}(1680)$	1.685	0.119
$\bar{\Delta}^0(1700)$	1.7	0.117
$\Delta^+(1700)$	1.7	0.117
$K_2^{*-}(1430)$	1.4256	0.115
$\bar{\Delta}^-(1620)$	1.63	0.113
$\Delta^{++}(1620)$	1.63	0.113
$\Lambda(1520)$	1.5195	0.112
$\bar{\Lambda}(1520)$	1.5195	0.112
$K_2^{*0}(1430)$	1.4324	0.109
$\eta(1405)$	1.4103	0.104
$\bar{n}(1535)$	1.535	0.103
$p(1535)$	1.535	0.102
$\bar{n}(1700)$	1.7	0.102
$p(1700)$	1.7	0.102
$\bar{n}(1720)$	1.72	0.098
$p(1720)$	1.72	0.098
$\rho_3^0(1690)$	1.6888	0.097
$\pi^-(1300)$	1.3	0.093
$a_0^-(1450)$	1.474	0.091
$\bar{p}(1520)$	1.52	0.088
		95%
$n(1520)$	1.52	0.088
$\bar{\Delta}^0(1620)$	1.63	0.086
$\Delta^+(1620)$	1.63	0.086
$\pi_2^+(1670)$	1.6724	0.086

TABLE III. Resonance contribution list for  $\pi^+$ , for  $T_{\text{conv}} = 120 \text{ MeV}$  (continued).

name	mass (GeV)	total contribution (%)	
$\rho^0(1450)$	1.465	0.082	
$\rho^+(1450)$	1.465	0.082	
$\pi_1^-(1400)$	1.376	0.08	
$\pi_1^0(1400)$	1.376	0.08	
$\bar{\Sigma}^-(1670)$	1.67	0.079	
$\Sigma^+(1670)$	1.67	0.079	
$\Sigma^+(1775)$	1.775	0.075	
$\bar{\Sigma}^-(1775)$	1.775	0.075	
$\rho^+(1700)$	1.72	0.072	
$n(1700)$	1.7	0.072	
$\bar{p}(1700)$	1.7	0.072	
$n(1440)$	1.44	0.072	
$\bar{p}(1440)$	1.44	0.072	
$\Delta^0(1700)$	1.7	0.07	
$\bar{\Delta}^+(1700)$	1.7	0.07	
$\Lambda(1690)$	1.69	0.069	
$\bar{\Lambda}(1690)$	1.69	0.069	
$\Sigma^0(1385)$	1.3837	0.069	
$\bar{\Sigma}^0(1385)$	1.3837	0.069	
$\omega(1650)$	1.67	0.067	
$n(1675)$	1.675	0.061	
$\bar{p}(1675)$	1.675	0.061	
$\pi_1^+(1600)$	1.653	0.06	
$\bar{K}_2^0(1770)$	1.773	0.056	
$K_2^+(1770)$	1.773	0.056	
$\Sigma^0(1670)$	1.67	0.05	
$\bar{\Sigma}^0(1670)$	1.67	0.05	
$\bar{\Delta}^-(1905)$	1.89	0.05	
$\Delta^{++}(1905)$	1.89	0.05	
$\rho^0(1700)$	1.72	0.049	
$\Delta^0(1620)$	1.63	0.048	
$\bar{\Delta}^+(1620)$	1.63	0.048	
$\pi_2^0(1670)$	1.6724	0.045	
$\bar{n}(1710)$	1.71	0.044	
$\bar{\Delta}^0(1905)$	1.89	0.044	
$K_0^{*+}(1430)$	1.412	0.044	
$\Delta^+(1905)$	1.89	0.044	
$p(1710)$	1.71	0.044	
$\bar{K}_0^{*0}(1430)$	1.412	0.044	
$\bar{\Sigma}^-(1660)$	1.66	0.043	
$\Sigma^+(1660)$	1.66	0.043	
$\bar{n}(1650)$	1.655	0.042	
$p(1650)$	1.655	0.042	
$f_0(1500)$	1.507	0.041	
$\eta(1475)$	1.476	0.04	98%
$\bar{\Delta}^-(1950)$	1.93	0.04	
$\Delta^{++}(1950)$	1.93	0.04	
$\bar{\Delta}^-(1920)$	1.92	0.039	

TABLE IV. Resonance contribution list for  $\pi^+$ , for  $T_{\text{conv}} = 120 \text{ MeV}$  (continued).

name	mass (GeV)	total contribution (%)
$\Delta^{++}(1920)$	1.92	0.039
$\Lambda(1830)$	1.83	0.037
$\bar{\Lambda}(1830)$	1.83	0.037
$\rho_3^-(1690)$	1.6888	0.037
$\bar{K}_3^{*0}(1780)$	1.776	0.034
$K_3^{*+}(1780)$	1.776	0.034
$\rho^-(1700)$	1.72	0.034
$n(1535)$	1.535	0.033
$\bar{p}(1535)$	1.535	0.033
$n(1720)$	1.72	0.033
$\bar{p}(1720)$	1.72	0.033
$\bar{p}(1680)$	1.685	0.032
$n(1680)$	1.685	0.032
$K_2^0(1770)$	1.773	0.032
$\bar{K}_2^0(1820)$	1.816	0.032
$K_2^-(1770)$	1.773	0.032
$K_2^+(1820)$	1.816	0.032
$\pi_2^-(1670)$	1.6724	0.031
$\Lambda(1600)$	1.6	0.03
$\bar{\Lambda}(1600)$	1.6	0.03
$f_0(1370)$	1.4	0.029
$\Delta^0(1905)$	1.89	0.028
$\bar{\Delta}^+(1905)$	1.89	0.028
$n(1710)$	1.71	0.027
$\bar{p}(1710)$	1.71	0.027
$\phi(1680)$	1.68	0.026
$\bar{\Delta}^0(1950)$	1.93	0.024
$\Delta^+(1950)$	1.93	0.024
		99%
$K^{*+}(1680)$	1.717	0.024
$\bar{K}^{*0}(1680)$	1.717	0.024
$\pi_1^-(1600)$	1.653	0.024
$\pi_1^0(1600)$	1.653	0.024
$\bar{\Sigma}^-(1915)$	1.915	0.023
$\Sigma^+(1915)$	1.915	0.023
$\bar{\Delta}^0(1920)$	1.92	0.023
$\Delta^+(1920)$	1.92	0.023
$\Xi^0(1820)$	1.823	0.023
$\bar{\Xi}^-(1820)$	1.823	0.023
$\bar{\Sigma}^-(1940)$	1.94	0.022
$\Sigma^+(1940)$	1.94	0.022
$\Lambda(1670)$	1.67	0.021
$\bar{\Lambda}(1670)$	1.67	0.021
$\bar{\Delta}^-(1910)$	1.91	0.02
$\Delta^{++}(1910)$	1.91	0.02
$\Sigma^0(1775)$	1.775	0.02
$\bar{\Sigma}^0(1775)$	1.775	0.02
$K_2^0(1820)$	1.816	0.019
$K_2^-(1820)$	1.816	0.019
$\bar{\Delta}^-(1930)$	1.96	0.017
$\Delta^{++}(1930)$	1.96	0.017

TABLE V. Resonance contribution list for  $\pi^+$ , for  $T_{\text{conv}} = 120 \text{ MeV}$  (continued).

name	mass (GeV)	total contribution (%)
$f'_2(1525)$	1.525	0.015
$\Sigma^0(1660)$	1.66	0.014
$\bar{\Sigma}^0(1660)$	1.66	0.014
$\bar{\Sigma}^-(1750)$	1.75	0.014
$\Sigma^+(1750)$	1.75	0.014
$\Sigma^0(1750)$	1.75	0.014
$\bar{\Sigma}^0(1750)$	1.75	0.014
$K_3^{*0}(1780)$	1.776	0.014
$K_3^{*-}(1780)$	1.776	0.014
$f_2(2010)$	2.011	0.012
$\Delta^-(1600)$	1.6	0.012
$\bar{\Delta}^{++}(1600)$	1.6	0.012
$\Lambda(1890)$	1.89	0.011
$\bar{\Lambda}(1890)$	1.89	0.011
$\Delta^0(1920)$	1.92	0.011
$\bar{\Delta}^+(1920)$	1.92	0.011
$\bar{\Delta}^0(1910)$	1.91	0.011
$\Delta^+(1910)$	1.91	0.011
$\Delta^0(1950)$	1.93	0.011
$\bar{\Delta}^+(1950)$	1.93	0.011
$\Lambda(1820)$	1.82	0.011
$\bar{\Lambda}(1820)$	1.82	0.011
$\pi^+(1800)$	1.812	0.01
$\Lambda(1800)$	1.8	0.01
$\bar{\Lambda}(1800)$	1.8	0.01
$\Sigma^0(1940)$	1.94	0.009
$\bar{\Sigma}^0(1940)$	1.94	0.009
$\Sigma^-(1750)$	1.75	0.009
$\bar{\Sigma}^+(1750)$	1.75	0.009
$\Sigma^0(1915)$	1.915	0.009
$\bar{\Sigma}^0(1915)$	1.915	0.009
$\bar{\Xi}^0(1820)$	1.823	0.009
$\Xi^-(1820)$	1.823	0.009
$\Xi^0(1950)$	1.95	0.008
$\bar{\Xi}^-(1950)$	1.95	0.008
$\Lambda(1810)$	1.81	0.008
$\bar{\Lambda}(1810)$	1.81	0.008
$K^{*-}(1680)$	1.717	0.007
$K^{*0}(1680)$	1.717	0.007
$\bar{\Sigma}^+(1775)$	1.775	0.007
$\Sigma^-(1775)$	1.775	0.006
$\bar{\Delta}^0(1930)$	1.96	0.006
$\Delta^+(1930)$	1.96	0.006
$\Omega(2250)$	2.252	0.006
$\Delta^0(1910)$	1.91	0.005
$\bar{\Delta}^+(1910)$	1.91	0.005
$n(1650)$	1.655	0.005
$\bar{p}(1650)$	1.655	0.005

TABLE VI. Resonance contribution list for  $\pi^+$ , for  $T_{\text{conv}} = 120 \text{ MeV}$  (continued).

name	mass (GeV)	total contribution (%)	
$\pi^-(1800)$	1.812	0.004	
$\pi^0(1800)$	1.812	0.004	
$\phi_3(1850)$	1.854	0.004	
$f_2(1950)$	1.945	0.003	
$\Delta^-(1920)$	1.92	0.003	
$\bar{\Delta}^{++}(1920)$	1.92	0.003	
$f_0(1710)$	1.715	0.002	
$\Delta^-(1910)$	1.91	0.002	
$\bar{\Delta}^{++}(1910)$	1.91	0.002	
$\Sigma^-(1940)$	1.94	0.001	
$\bar{\Sigma}^+(1940)$	1.94	0.001	
$\Sigma^-(1915)$	1.915	0	
$\bar{\Sigma}^+(1915)$	1.915	0	100%

TABLE VII. Resonance contribution list for  $\pi^+$ , for  $T_{\text{conv}} = 120 \text{ MeV}$  (continued).

name	mass (GeV)	total contribution (%)	
$K^{*0}(892)$	0.8961	35.857	
$K^{*+}(892)$	0.89166	18.52	
$\phi(1020)$	1.0195	16.036	60%
$K_1^+(1270)$	1.273	3.631	
$K_1^0(1270)$	1.273	3.287	
$a_0^+(980)$	0.9847	1.807	
$f_1(1420)$	1.4263	1.754	80%
$K_2^{*0}(1430)$	1.4324	1.61	
$K_1^+(1400)$	1.402	1.446	
$K_2^{*+}(1430)$	1.4256	1.241	
$K^{*+}(1410)$	1.414	1.217	
$K_1^0(1400)$	1.402	1.127	
$K^{*0}(1410)$	1.414	1.033	
$a_0^0(980)$	0.9847	0.898	
$f_0(980)$	0.9741	0.869	90%
$\bar{\Lambda}(1520)$	1.5195	0.798	
$f'_2(1525)$	1.525	0.711	
$f_1(1285)$	1.2818	0.493	
$\bar{\Xi}^-(1690)$	1.69	0.462	
$\bar{\Sigma}^-(1775)$	1.775	0.431	
$\eta(1475)$	1.476	0.405	
$K_0^{*0}(1430)$	1.412	0.295	
$\bar{\Xi}^-(1820)$	1.823	0.288	
$a_2^+(1320)$	1.3183	0.274	
$\eta(1405)$	1.4103	0.265	
$\phi(1680)$	1.68	0.265	95%
$f_2(2010)$	2.011	0.259	
$\bar{\Sigma}^0(1775)$	1.775	0.237	
$\bar{\Xi}^0(1690)$	1.69	0.23	
$\bar{\Lambda}(1820)$	1.82	0.196	
$K_3^{*+}(1780)$	1.776	0.191	
$K_2^+(1770)$	1.773	0.189	
$\bar{\Sigma}^-(1670)$	1.67	0.177	
$\bar{\Sigma}^-(1750)$	1.75	0.171	
$K_2^0(1770)$	1.773	0.166	
$\bar{\Sigma}^-(1660)$	1.66	0.165	
$\bar{\Lambda}(1600)$	1.6	0.161	
$\eta(1295)$	1.294	0.157	
$K_0^{*+}(1430)$	1.412	0.148	
$K_2^+(1820)$	1.816	0.145	
$\bar{\Lambda}(1690)$	1.69	0.144	
$K_3^{*0}(1780)$	1.776	0.14	
$a_2^0(1320)$	1.3183	0.137	98%
$K^{*0}(1680)$	1.717	0.117	

TABLE VIII. Resonance contribution list for  $K^+$ , for  $T_{\text{conv}} = 120 \text{ MeV}$ .

name	mass (GeV)	total contribution (%)	
$\phi_3(1850)$	1.854	0.114	
$f_2(1270)$	1.2754	0.099	
$\bar{\Lambda}(1810)$	1.81	0.091	
$\bar{\Sigma}^0(1670)$	1.67	0.089	
$\bar{\Lambda}(1890)$	1.89	0.087	
$\bar{\Sigma}^0(1750)$	1.75	0.085	
$\bar{\Sigma}^0(1660)$	1.66	0.082	
$K_2^0(1820)$	1.816	0.082	
$\bar{\Xi}^-(1950)$	1.95	0.082	
$\bar{\Lambda}(1670)$	1.67	0.082	99%
$K^{*+}(1680)$	1.717	0.078	
$\bar{\Lambda}(1800)$	1.8	0.076	
$p(1720)$	1.72	0.072	
$p(1710)$	1.71	0.068	
$\eta_2(1645)$	1.617	0.06	
$\bar{\Xi}^0(1820)$	1.823	0.052	
$a_0^+(1450)$	1.474	0.052	
$\bar{\Sigma}^+(1940)$	1.94	0.047	
$\bar{\Sigma}^0(1940)$	1.94	0.045	
$\bar{\Omega}(2250)$	2.252	0.044	
$\bar{\Sigma}^+(1775)$	1.775	0.043	
$\bar{\Sigma}^-(1940)$	1.94	0.043	
$\bar{\Sigma}^-(1915)$	1.915	0.036	
$p(1650)$	1.655	0.032	
$a_0^0(1450)$	1.474	0.026	
$f_0(1710)$	1.715	0.024	
$\rho_3^+(1690)$	1.6888	0.023	
$\bar{\Sigma}^0(1915)$	1.915	0.018	
$\bar{\Lambda}(1830)$	1.83	0.017	
$\rho_3^0(1690)$	1.6888	0.016	
$\pi_2^+(1670)$	1.6724	0.015	
$\pi_2^0(1670)$	1.6724	0.013	
$f_0(1500)$	1.507	0.012	
$\pi_2^-(1670)$	1.6724	0.01	
$f_0(1370)$	1.4	0.01	
$\rho_3^-(1690)$	1.6888	0.008	
$\Delta^{++}(1920)$	1.92	0.004	
$\Delta^+(1920)$	1.92	0.003	
$\Delta^{++}(1950)$	1.93	0.003	
$\Delta^+(1950)$	1.93	0.002	
$\bar{K}_1^0(1400)$	1.402	0.002	
$K_1^-(1400)$	1.402	0.002	
$\Delta^0(1920)$	1.92	0.001	
$f_2(1950)$	1.945	0.001	
$\Delta^0(1950)$	1.93	0.001	
$\bar{K}_2^0(1820)$	1.816	0	
$K_2^-(1820)$	1.816	0	100%

TABLE IX. Resonance contribution list for  $K^+$ , for  $T_{\text{conv}} = 120 \text{ MeV}$  (continued).

name	mass (GeV)	total contribution (%)	
$\Delta^{++}(1232)$	1.232	29.842	
$\Delta^+(1232)$	1.232	19.816	
$\Delta^0(1232)$	1.232	9.813	
$\Delta^{++}(1600)$	1.6	2.787	60%
$n(1520)$	1.52	2.487	
$p(1520)$	1.52	2.169	
$\Delta^+(1600)$	1.6	2.049	
$p(1440)$	1.44	2.034	
$n(1440)$	1.44	1.943	
$p(1535)$	1.535	1.452	
$\Delta^{++}(1700)$	1.7	1.386	
$\Lambda(1520)$	1.5195	1.365	
$p(1675)$	1.675	1.347	
$\Delta^0(1600)$	1.6	1.314	
$p(1700)$	1.7	1.228	80%
$\Delta^{++}(1620)$	1.63	1.135	
$n(1680)$	1.685	1.003	
$\Delta^+(1700)$	1.7	0.987	
$n(1675)$	1.675	0.975	
$p(1680)$	1.685	0.917	
$n(1535)$	1.535	0.793	
$\Delta^+(1620)$	1.63	0.785	
$n(1720)$	1.72	0.752	
$\Sigma^+(1775)$	1.775	0.738	
$\Delta^-(1600)$	1.6	0.574	
$\Delta^0(1700)$	1.7	0.54	90%
$\Delta^{++}(1905)$	1.89	0.536	
$p(1720)$	1.72	0.487	
$p(1710)$	1.71	0.456	
$\Delta^0(1620)$	1.63	0.433	
$n(1650)$	1.655	0.429	
$\Delta^{++}(1950)$	1.93	0.411	
$\Sigma^0(1775)$	1.775	0.405	
$\Delta^+(1905)$	1.89	0.366	
$n(1700)$	1.7	0.342	
$\Lambda(1820)$	1.82	0.334	
$\Sigma^+(1670)$	1.67	0.302	
$p(1650)$	1.655	0.29	95%
$\Sigma^+(1750)$	1.75	0.289	
$\Sigma^+(1660)$	1.66	0.282	
$\Delta^+(1950)$	1.93	0.281	
$\Lambda(1600)$	1.6	0.275	
$\Lambda(1690)$	1.69	0.247	
$\Delta^{++}(1920)$	1.92	0.227	
$n(1710)$	1.71	0.203	
$\Delta^{++}(1930)$	1.96	0.196	
$\Delta^0(1905)$	1.89	0.189	
$\Delta^+(1920)$	1.92	0.182	

TABLE X. Resonance contribution list for  $p$ , for  $T_{\text{conv}} = 120 \text{ MeV}$ .

name	mass (GeV)	total contribution (%)	
$\Lambda(1810)$	1.81	0.156	
$\Delta^0(1950)$	1.93	0.153	
$\Sigma^0(1670)$	1.67	0.151	
$\Lambda(1890)$	1.89	0.15	98%
$\Sigma^0(1750)$	1.75	0.145	
$\Sigma^0(1660)$	1.66	0.141	
$\Lambda(1670)$	1.67	0.139	
$\Sigma^+(1940)$	1.94	0.138	
$\Delta^0(1920)$	1.92	0.137	
$\Delta^-(1700)$	1.7	0.136	
$\Delta^+(1930)$	1.96	0.13	
$\Lambda(1800)$	1.8	0.13	99%
$\Delta^{++}(1910)$	1.91	0.121	
$\Delta^+(1910)$	1.91	0.096	
$\Delta^-(1920)$	1.92	0.092	
$\Delta^-(1620)$	1.63	0.081	
$\Sigma^0(1940)$	1.94	0.077	
$\Sigma^-(1775)$	1.775	0.074	
$\Delta^0(1910)$	1.91	0.071	
$\Delta^0(1930)$	1.96	0.065	
$\Sigma^+(1915)$	1.915	0.062	
$\Delta^-(1910)$	1.91	0.046	
$\Sigma^0(1915)$	1.915	0.031	
$\Lambda(1830)$	1.83	0.029	
$\Delta^-(1950)$	1.93	0.023	
$\Delta^-(1905)$	1.89	0.016	
$\Sigma^-(1940)$	1.94	0.015	100%

TABLE XI. Resonance contribution list for  $p$ , for  $T_{\text{conv}} = 120 \text{ MeV}$  (continued).

name	mass (GeV)	total contribution (%)	
$\Sigma^0$	1.1926	24.775	
$\Sigma^+(1385)$	1.3828	17.893	
$\Sigma^-(1385)$	1.3872	17.346	60%
$\Sigma^0(1385)$	1.3837	16.555	
$\Lambda(1405)$	1.4065	3.103	
$\Lambda(1520)$	1.5195	2.18	80%
$\Sigma^-(1670)$	1.67	1.304	
$\Sigma^+(1670)$	1.67	1.297	
$\Lambda(1690)$	1.69	1.178	
$\Xi^-(1690)$	1.69	1.132	
$\Xi^0(1690)$	1.69	1.128	
$\Sigma^+(1775)$	1.775	0.771	
$\Sigma^-(1775)$	1.775	0.769	
$\Lambda(1830)$	1.83	0.754	90%
$\Sigma^0(1775)$	1.775	0.749	
$\Sigma^-(1660)$	1.66	0.708	
$\Sigma^+(1660)$	1.66	0.707	
$\Xi^0(1820)$	1.823	0.707	
$\Xi^-(1820)$	1.823	0.705	
$\Sigma^0(1750)$	1.75	0.619	
$\Lambda(1670)$	1.67	0.607	
$\Lambda(1600)$	1.6	0.486	95%
$\Sigma^0(1670)$	1.67	0.485	
$\Sigma^0(1660)$	1.66	0.471	
$\Sigma^-(1915)$	1.915	0.382	
$\Sigma^+(1915)$	1.915	0.381	
$\Sigma^0(1915)$	1.915	0.264	
$\Lambda(1820)$	1.82	0.216	
$\Xi^0(1950)$	1.95	0.202	
$\Xi^-(1950)$	1.95	0.201	98%
$\Sigma^-(1940)$	1.94	0.189	
$\Sigma^+(1940)$	1.94	0.188	
$n(1720)$	1.72	0.176	
$p(1720)$	1.72	0.176	
$\Lambda(1890)$	1.89	0.174	
$n(1710)$	1.71	0.167	99%
$p(1710)$	1.71	0.167	
$\Sigma^0(1940)$	1.94	0.155	
$\Lambda(1800)$	1.8	0.155	
$n(1650)$	1.655	0.078	
$p(1650)$	1.655	0.078	
$\Sigma^-(1750)$	1.75	0.076	
$\Sigma^+(1750)$	1.75	0.075	
$\Lambda(1810)$	1.81	0.05	
$\Delta^0(1920)$	1.92	0.007	
$\Delta^+(1920)$	1.92	0.007	
$\Delta^0(1950)$	1.93	0.004	
$\Delta^+(1950)$	1.93	0.004	100%

TABLE XII. Resonance contribution list for  $\Lambda$ , for  $T_{\text{conv}} = 120 \text{ MeV}$ .

name	mass (GeV)	total contribution (%)	
$\Lambda(1405)$	1.4065	25.159	
$\Lambda(1520)$	1.5195	10.121	
$\Sigma^+(1385)$	1.3828	9.288	
$\Sigma^0(1385)$	1.3837	9.179	
$\Sigma^0(1670)$	1.67	6.648	60%
$\Sigma^+(1670)$	1.67	6.618	
$\Xi^0(1690)$	1.69	4.578	
$\Sigma^+(1750)$	1.75	4.425	
$\Lambda(1600)$	1.6	3.969	
$\Lambda(1690)$	1.69	3.845	80%
$\Lambda(1830)$	1.83	2.243	
$\Lambda(1670)$	1.67	1.926	
$\Sigma^+(1660)$	1.66	1.916	
$\Sigma^0(1660)$	1.66	1.916	90%
$\Xi^0(1820)$	1.823	1.045	
$\Sigma^+(1915)$	1.915	0.974	
$\Sigma^0(1915)$	1.915	0.968	
$\Sigma^+(1775)$	1.775	0.859	95%
$\Sigma^0(1775)$	1.775	0.805	
$\Lambda(1820)$	1.82	0.791	
$\Sigma^-(1775)$	1.775	0.6	
$\Sigma^+(1940)$	1.94	0.405	98%
$\Lambda(1810)$	1.81	0.402	
$\Sigma^0(1940)$	1.94	0.387	99%
$\Lambda(1800)$	1.8	0.377	
$\Lambda(1890)$	1.89	0.231	
$\Sigma^-(1940)$	1.94	0.101	
$\Delta^{++}(1920)$	1.92	0.08	
$\Delta^{++}(1950)$	1.93	0.051	
$\Delta^+(1920)$	1.92	0.027	
$\Sigma^-(1750)$	1.75	0.02	
$\Sigma^0(1750)$	1.75	0.02	
$\Delta^+(1950)$	1.93	0.015	
$\Sigma^-(1915)$	1.915	0.007	100%

TABLE XIII. Resonance contribution list for  $\Sigma^+$ , for  $T_{\text{conv}} = 120 \text{ MeV}$ .

name	mass (GeV)	total contribution (%)	
$\Xi^0(1530)$	1.5318	62.049	60%
$\Xi^-(1530)$	1.535	30.103	90%
$\Xi^0(1820)$	1.823	2.42	
$\Xi^-(1820)$	1.823	2.334	95%
$\Xi^0(1950)$	1.95	1.427	98%
$\Omega(2250)$	2.252	0.957	99%
$\Xi^-(1950)$	1.95	0.71	100%

TABLE XIV. Resonance contribution list for  $\Xi^-$ , for  $T_{\text{conv}} = 120 \text{ MeV}$ .